Astron. Astrophys. 356, 238–252 (2000)

ASTRONOMY AND ASTROPHYSICS

Abundances of light elements in metal-poor stars⋆

III. Data analysis and results

E. Carretta[1], **R.G. Gratton**[1], **and C. Sneden**[2]

[1] Osservatorio Astronomico di Padova, Vicolo dell'Osservatorio 5, 35122 Padova, Italy
[2] University of Texas at Austin and McDonald Observatory, USA

Received 17 January 2000 / Accepted 17 February 2000

Abstract. We present the results of the analysis of an extensive set of new and literature high quality data concerning Fe, C, N, O, Na, and Mg. This analysis exploited the $T_{\rm eff}$ scale determined in Gratton et al. (1996a), and the non-LTE abundance corrections computed in Gratton et al. (1999a). Results obtained with various abundance indices are discussed and compared. Detailed comparison with models of galactic chemical evolution will be presented in future papers of this series.

Our non-LTE analysis yields the same O abundances from both permitted and forbidden lines for stars with $T_{\rm eff}$ >4600 K, in agreement with King (1993), but not with other studies using a lower $T_{\rm eff}$ -scale for subdwarfs. However, we obtain slightly smaller O abundances for the most luminous metal-poor field stars than for fainter stars of similar metallicities, an effect attributed to inadequacies of the adopted model atmospheres (Kurucz 1992, with overshooting) for cool stars. We find a nearly constant O overundance in metal-poor stars ([Fe/H]< -0.8), at a mean value of 0.46 ± 0.02 dex ($\sigma = 0.12$, 32 stars), with only a gentle slope with [Fe/H] (~ -0.1); this result is different from the steeper slope recently obtained using OH band in the near UV.

If only *bonafide* unmixed stars are considered, C abundances scale with Fe ones (i.e. [C/Fe]≈ 0) down to [Fe/H]~ -2.5. Due to our adoption of a different $T_{\rm eff}$ scale, we do not confirm the slight C excess in the most metal poor disk dwarfs ($-0.8 <$[Fe/H]< -0.4) found in previous investigations.

Na abundances scale as Fe ones in the high metallicity regime, while metal-poor stars present a Na underabundance. None of the field stars analyzed belong to the group of O-poor and Na-rich stars observed in globular clusters. Na is deficient with respect to Mg in halo and thick disk stars; within these populations, Na deficiency may be a slow function of [Mg/H]. Solar [Na/Mg] ratios are obtained for thin disk stars.

Key words: stars: abundances – nuclear reactions, nucleosynthesis, abundances – Galaxy: evolution

1. Introduction

The abundances of light elements (CNO, Na and Mg) in metal-poor stars provide basic constraints for models of the chemical evolution of our Galaxy. These elements are produced by different mechanisms in various astronomical sites. The ejecta of core collapse SNe are expected to be very rich in O, while they are expected to contribute only a fraction of the present C content of the interstellar medium (ISM) (see e.g. Woosley & Weaver 1986, 1995; Timmes et al. 1995; Thielemann et al. 1990). On the other hand, mixing and/or severe mass loss may bring to the surface large amounts of freshly synthesized C from the outer and cooler regions of He-burning shells; this C may then be returned to the ISM by stellar winds (Iben & Renzini 1983 and references therein). Since these are not fully understood mechanisms, and they may be active in stars of very different masses (and hence lifetimes), the run of the [C/Fe] ratio with time or overall metal abundance [Fe/H] [1] is presently not well constrained by stellar and galactic evolution models. Much more insight can be gained from observations.

Even more intriguing is the case for N, since this element is not directly produced in large amounts by hydrostatic He-burning; N synthesis requires recycling of material from a region where H-burning occurs through the CNO cycle. In the case of massive stars, N synthesis is then expected to be a secondary process (see e.g. Woosley & Weaver 1995), although under certain circumstances even a primary behaviour could be obtained (Timmes et al. 1995). Observational data indicate that large amounts of N are present in the outer layers of evolved stars over a wide mass range. From there, N can be lost to the ISM through quiescent or violent stellar winds, as e.g. in the case of planetary nebulae. This N might result from the processing of either the original C (leading to a secondary-like behaviour), or of freshly synthesized ^{12}C as a consequence of CN-cycle hydrogen-burning at the base of the outer convective envelope which penetrates inward in regions where He-burning

Send offprint requests to: E. Carretta

⋆ Tables 2 to 9 are only available in electronic form at the CDS via anonymous ftp to cdsarc.u-strasbg.fr (130.79.128.5) or via http://cdsweb.u-strabg.fr/Abstract.html

[1] In this paper we will use two different notations for abundances: log n(A) is the abundance (by number) of the element A in the usual scale where log n(H)=12; [A/H] is the logarithmic ratio of the abundances of elements A and H in the star, minus the same quantity in the Sun.

previously occurred during the interpulse phases in thermally pulsing intermediate mass stars (hot bottomed convective envelopes: Truran & Cameron 1971; Pagel & Edmunds 1981). In this case N-synthesis has a primary-like behaviour. Lack of an adequate knowledge of the relevant mechanisms prevents accurate predictions of the run of the [N/Fe] ratio with metal abundance.

The production of Mg (and other α-elements like Si, S, Ca, and Ti) closely mimics the production of O, replacing hydrostatic He-burning with hydrostatic burning of C (or O, etc.). Core collapse SN explosions of massive stars are expected to return to the ISM large amounts of Mg (Thielemann et al. 1990; Tsujimoto et al. 1995; Woosley & Weaver 1995).

Finally, Na production during C-burning in massive stars is primary, it is a rather strong function of the neutron density (Truran & Arnett 1971; Woosley & Weaver 1995); since this is expected to be a function of initial stellar metallicity, the [Na/Mg] ratio is predicted to fall below solar in metal-poor stars (Arnett 1973; Truran 1973; Woosley & Weaver 1995). It should however be noted that Na synthesis by p-capture on ^{22}Ne in regions of H-burning shell where O is converted into N has been claimed to explain the Na excesses observed in supergiants and in bright giants in globular clusters (Denisenkov & Denisenkova 1990); Woosley & Weaver (1995) predicts that some 10% of the ^{23}Na synthesized in massive stars is produced in the H-envelope as consequence of the Ne-Na cycle. The effects of this reaction during the RGB phase of small mass stars have been studied in detail by Langer et al. (1993). These authors found that also a ^{20}Ne-^{23}Na cycle might perhaps occur in these stars; given the large abundances of this last Ne isotope, this reaction might well explain observed Na excesses. It is now clear that the Na-O anticorrelation is confined to the large density environments of globular clusters (see e.g. Gratton et al. 2000a). However no study of the impact of the possible production of Na in small mass stars on galactic chemical evolution is available.

Observational evidences concerning these elements are discussed in a number of reviews (see e.g. Wheeler et al. 1989). In the following, we will only recall the most important points and give some updates. The situation for C and N is rather confusing due to difficulties in observing the few good abundance indices in metal-poor stars, and to the occurrence of mixing in evolved stars. A variety of spectral indices can be considered for C and N: however, most of them cannot be used over a wide range of metal abundances. This is the case of C_2 and CN lines, whose strengths depend approximately quadratically on metal abundance (neglecting the variation of the gaseous pressure with metallicity): their observation is limited to evolved and/or metal rich stars. Several permitted lines of both C and N are observable in the optical and near-IR; however, they are of high excitation and the possible presence of departures from LTE should be carefully considered for the strongest features (see e.g. Tomkin et al. 1992). The forbidden [CI] line at 8727 Å (a high quality abundance indicator in the Sun) is vanishingly weak in metal-poor stars. Good data are provided by CH; unluckily, the best bands of NH are in the near UV, in a quite difficult spectral region. Furthermore, basic data about dissociation and pre-dissociation are not accurately determined for these molecules (see Lambert 1978), causing offsets to be present among various abundance determinations. With these caveats in mind, it is not surprising that there are rather large uncertainties in presently determined trends with metal abundance: current data suggests that the abundances of both C (Peterson & Sneden 1978; Clegg et al. 1981; Laird 1985) and N (Clegg et al. 1981; Tomkin & Lambert 1984; Laird 1985; Carbon et al. 1987) scale as the Fe one, with a possible upward trend for C in the most metal-poor stars (Tomkin et al. 1986; Carbon et al. 1987; Tomkin et al. 1992). The presence of a moderate trend for decreasing [C/Fe] ratios with increasing [Fe/H] amongst disk stars ([Fe/H]> -1) has been recently proposed by Andersson & Edvardsson (1994) and Tomkin et al. (1995) from observations of forbidden and permitted C lines respectively.

The run of O abundances with overall metallicity has been the topic of a rather large number of papers in the recent past. A nearly constant [O/Fe] ratio at [O/Fe]$\sim +0.4$ has been indicated by studies of the forbidden line at 6300 Å in metal-poor giants (Gratton & Ortolani 1986; Barbuy 1988; Barbuy & Erdelyi-Mendes 1989; Sneden et al. 1991; Kraft et al. 1992). A nearly constant offset of the abundances of O could be interpreted as the result of the contribution by type II SNe alone to the early galactic nucleosynthesis (see e.g. Matteucci & Greggio 1986). Larger O excesses have been obtained from the analysis of the near IR permitted lines in metal-poor dwarfs (Sneden et al. 1979), with an even larger value ([O/Fe]~ 0.9) obtained by Abia & Rebolo (1989). This last analysis does not indicate any plateau in the run of [O/Fe] with [Fe/H], suggesting that only the ejecta of the most massive among type II SNe polluted the medium from which early stars formed, and requiring then a very fast raise of the metal abundance. Additional important results have been obtained exploiting OH lines at the UV edge of ground-based and in the near IR spectra of subdwarfs; note that use of OH bands is very promising, since these are detectable also in extremely metal-poor stars, where the other diagnostics are vanishingly weak. Early results (Bessell et al. 1991; Balachandran & Carney 1996) seemed to confirm those obtained from forbiden lines. However, more extensive analysis (Nissen et al. 1994; Israelian et al. 1998; Boesgaard et al. 1999) are in better agreement with results from the permitted lines. If these large O abundances held for globular clusters too, the deduced ages would be substantially reduced.

An examination of these O abundance analyses reveals several weak points. (i) A Na-O anticorrelation exists amongst the brightest globular cluster giants (see Kraft 1994 and references therein), although its explanation is still not clear. In a very recent analysis of mixing episodes amongst field stars (Gratton et al. 2000a), we find that deep mixing (affecting C and N abundances) indeed occurs at luminosities brighter than the RGB bump, when the molecular weight barrier is canceled by the outward expansion of the H-burning shell. However, O (and Na) abundances are unaltered in field stars, in good agreement with predictions of theoretical models (Sweigart & Mengel 1979; Charbonnel 1994), and previous observational indications (Kraft et al. 1982, Shetrone 1996, Pilachowski et al. 1996, Kraft

et al. 1997). Hence the Na-O anticorrelation seems to be limited to the dense environments of globular clusters, and not relevant for the discussion of field stars. (ii) O abundances are sensitive to the adopted atmospheric parameters. (iii) Permitted IR lines likely form in non-LTE conditions when lines are rather strong (Baschek et al. 1977), while no departure from LTE is expected for the forbidden line at 6300.3 Å. A very critical test would thus be the analysis of forbidden lines in very metal-poor dwarfs; unfortunately, this test can be done only for a few cool, not very metal-poor dwarfs and subgiants: results (Spiesmann & Wallerstein 1991; Spite & Spite 1991; Balachandran & Carney 1996; Fulbright & Kraft 1999) support the abundances obtained for giants. (iv) The UV OH bands used by Israelian et al. (1998) and Boesgaard et al. (1999) are in a very crowded region in the extreme ground-based UV, and oscillator strengths for these bands are not well determined: hence, results from OH cannot be still considered as conclusive (see also Balachandran & Bell 1997).

The problem of O abundances in metal-poor stars has been addressed in a series of papers by King (1993, 1994). He showed that while departures from LTE likely play only a minor rôle (a result also suggested by the statistical equilibrium computations by Kiselman 1991, 1993), abundances from permitted and forbidden lines both yield the same [O/Fe] ratio ([O/Fe]$\sim +0.5$, with only a shallow trend with overall metal abundance) if a new set of effective temperatures is adopted for subdwarfs and only high quality equivalent widths (EWs) are used. Unfortunately, the temperature scale for subdwarfs is still not well settled: temperatures derived by at least one recent paper (Nissen et al. 1994) are much lower than those adopted by King (1993); adoption of these low temperatures would regenerate the very high O abundances found in older analyses of subdwarfs (see Cavallo et al. 1997).

Abundances for Na and Mg in metal-poor stars have been determined by a number of authors (François 1986a, 1986b; Magain 1987; Gratton & Sneden 1987, 1988). However fine details, like the possible existence of a gradient of [Mg/Fe] with [Fe/H] among stars with [Fe/H]< -1, or the precise form of the run of the [Na/Mg] ratio with [Fe/H], were still not defined in these older papers at the level required for a detailed comparison with the predictions by models of the chemical evolution of the Galaxy (se e.g. Matteucci & François 1992). In part, this is due to the rather large uncertainties present in the atmospheric parameters used by these otherwise careful discussions. For Mg, the situation has now changed thanks to the excellent papers by Fuhrmann et al. (1995), Fuhrmann (1998), and Nissen & Schuster (1997): these papers showed that (i) Mg is uniformly overabundant in most halo and all thick disk stars, although there are a few halo stars having lower Mg excesses; and (ii) the Fe abundance increase at constant Mg at the transition between thick and thin disk. This last result agrees with our earlier finding for O (Gratton et al. 1996b), and will be discussed more in detail in Paper IV.

The aim of the present series of papers is to contribute to the knowledge about the abundances of Fe, C, N, O, Na and Mg in metal-poor stars. In the course of this investigations, various critical points in the analysis were examined: some of them are discussed here, while others (the solar abundances and the applicability of Kurucz model atmospheres in abundance analyses) were considered in a parallel study of the spectra of RR Lyrae at minimum light (Clementini et al. 1995) and in a rather extensive comparison with solar observations (Castelli et al. 1997), in Gratton et al. (1996a: Paper I) (the $T_{\rm eff}$ scale and the adopted atmospheric parameters), and in Gratton et al. (1999a: Paper II) (non-LTE effects). In this paper we present the abundance analysis and its results. Detailed comparisons with nucleosynthesis predictions and models of galactic chemical evolution models will be done in forthcoming papers (Gratton et al. 2000b: Paper IV; Carretta & Gratton 2000a: Paper V). The observational material is described in Sect. 2, where we show its high degree of internal consistency, with the EWs generally accurate to within ± 2 mÅ. The abundance indicators used in the analysis, with the basic atomic and molecular data adopted, are described in Sect. 3. Our final abundances are presented in Sect. 4; for O, Mg and Na they include non-LTE corrections determined in Paper II. We found that our results have a high internal consistency, at least for $T_{\rm eff} > 4600$ K, with error bars in most cases below 0.1 dex. In particular, we obtain good agreement between abundances provided by low excitation, forbidden and high excitation, permitted O I lines; between C abundances deduced from C_2, CH, permitted and forbidden C I lines; and between Na abundances provided by the D and subordinate lines. Some problem still exists for Mg. We compare our results with those from some recent paper in Sect. 5; finally Conclusions are given in Sect. 6. Finally, note that the material on which the present analysis is based on does not include the data discussed in Gratton et al. (2000a).

2. Observational material

The observational material is described in paper I; here we recall that the original data concerning 19 metal-poor stars were complemented by literature data in order to better examine trends of abundances with [Fe/H] and luminosity. We considered selected data sets giving EWs for both neutral and ionized Fe lines, in order to derive gravities from ionization equilibrium for all stars. The following data sets were considered:

- Tomkin et al. (1992, hereinafter TLLS) analysis of high excitation, permitted C and O lines in 34 unvolved metal-poor stars.
- Sneden et al. (1991) and Kraft et al. (1992: hereinafter collectively SKPL) analysis of forbidden O and Na lines of field and cluster halo giants; for this data set we only considered here field stars (27 objects), owing to possible systematic differences between field and cluster stars.
- Edvardsson et al. (1993; hereinafter E93) analysis of permitted high excitation O, Na and Mg lines in 187 stars with [Fe/H]> -1. Data by E93 were complemented by those of Clegg et al. (1981), Andersson & Edvardsson (1994) and Tomkin et al. (1995) for C lines, and Nissen & Edvardsson (1992) for the [O I] forbidden lines in a smaller number of stars.

Table 1. Effects of errors in the atmospheric parameters for a metal-rich dwarf and a metal-poor giant

Element	Index	Δ $T_{\rm eff}$ +100K	Δ log g -0.5 dex	Δ[A/H] -0.2 dex	Δ v_t +0.5 km/s	Δ_{tot}	Δ(Sun)
HD 102365							
[Fe/H]	Fe I	0.10	-0.03	-0.04	-0.04	0.12	0.16
[Fe/H]	Fe II	-0.02	-0.30	-0.09	-0.04	0.32	0.04
[O/Fe]	[OI]	0.03	0.02	0.09	0.04	0.10	-0.05
[O/Fe]	OI	-0.07	0.11	0.11	0.03	0.17	-0.10
[C/Fe]	[CI]	0.01	0.09	0.02	0.04	0.10	-0.02
[C/Fe]	CI	-0.04	0.12	0.09	0.04	0.16	-0.10
[C/Fe]	CH	-0.05	-0.01	0.02	0.04	0.07	0.00
[C/Fe]	C2	-0.11	-0.09	0.04	0.04	0.15	-0.11
[N/Fe]	CN	-0.05	-0.06	0.05	0.04	0.10	-0.22
[Na/Fe]	Na I	-0.04	0.06	0.00	0.03	0.08	-0.04
[Mg/Fe]	4571	0.04	0.04	0.00	-0.01	0.06	-0.01
[Mg/Fe]	others	-0.05	0.02	0.01	0.04	0.07	-0.06
HD 122956							
[Fe/H]	Fe I	0.17	0.06	0.02	-0.21	0.21	
[Fe/H]	Fe II	-0.03	-0.17	-0.04	-0.11	0.18	
[O/Fe]	[OI]	0.03	-0.04	0.06	0.10	0.09	
[O/Fe]	OI	-0.10	-0.03	0.08	0.08	0.14	
[C/Fe]	CH	-0.13	-0.04	0.01	0.18	0.16	
[C/Fe]	C2	-0.17	-0.16	-0.01	0.21	0.26	
[N/Fe]	CN	-0.12	-0.19	-0.02	0.24	0.26	
[Na/Fe]	Na I	-0.10	-0.02	-0.01	0.20	0.14	
[Mg/Fe]	4571	0.08	0.02	0.03	-0.10	0.10	
[Mg/Fe]	others	-0.11	-0.03	-0.01	0.20	0.15	

– Zhao & Magain (1990, hereinafter ZM90) data for Na and Mg in 20 metal-poor dwarfs.

Atmospheric parameters for the program stars are given in Table 2 of Paper I. While data were obtained with different instrumentation and reduction procedures, the final set of EWs is highly homogenous. Mean differences between EWs determined on our original sample and those from literature are:

$$EW_{\rm us} - EW_{\rm E93} = 2.5 \pm 0.5 \ {\rm m\AA} \ (\sigma = 2.8 \ {\rm m\AA}),$$

$$EW_{\rm us} - EW_{\rm SKPL} = 2.4 \pm 0.6 \ {\rm m\AA} \ (\sigma = 3.5 \ {\rm m\AA}),$$

$$EW_{\rm us} - EW_{ZM90} = -0.4 \pm 0.7 \ {\rm m\AA} \ (\sigma = 3.3 \ {\rm m\AA}),$$

based on 21, 34 and 27 lines respectively. We did not apply any systematic corrections to the original EWs, and we estimate typical errors in individual EWs to be ± 2 mÅ.

3. Abundance indicators and analysis

Abundances were derived using model atmospheres extracted from the grid by Kurucz (1992; hereinafter K92)[2] and compared with solar ones obtained using the solar model atmosphere from the same grid, with a depth independent microturbulent velocity of $v_{\rm t}$=0.9 kms^{-1}(Simmons & Blackwell 1982). These solar abundances are very close to those obtained using the Holweger & Müller (1974) empirical solar model atmosphere (which is currently the best representation of solar photosphere), and to the meteoritic values listed by Anders & Grevesse (1989). Fe abundances are listed and discussed in Paper I; here, [Fe/H] values will be repeated only when needed.

CNO abundances were obtained using molecular concentrations given by a simultaneous solution of the dissociation equations for several species, following the method described in Lambert & Ries (1977, 1981). Coupling of atomic C and O concentrations due to CO formation is of particular relevance for C. We used O abundances given by the average of permitted and forbidden lines (see below). Furthermore, CN line strength depends on the product of the concentration of atomic C and N: hence, any change in the C abundance causes a corresponding modification in deduced N abundances. Corrections for CO formation are less important for O (since n(O)$\gg$n(C) in all program stars), the difference between abundances computed with [C/Fe]=0 or [C/Fe]$= -0.5$ being less than 0.05 dex in most cases. Given these interrelations among the various species, we will first present our results for O, and then discuss those for C and N.

Table 1 presents an analysis of the uncertainties on the derived abundances related to possible errors in the adopted atmospheric parameters. This was obtained by repeating the whole procedure of abundance derivations by modifying one parameter at a time for a couple of typical cases (a metal-rich dwarf

[2] CD-ROM 13; these models used here have the overshooting option switched on

and a metal-poor giant). Oxygen abundances were compared with those given by Fe II lines, in order to reduce their sensitivity on the adopted gravities. Column 7 of Table 1 lists a total uncertainty (due to possible errors in the atmospheric parameters); this was given by a quadratic sum of the effects of errors in the individual parameters[3]. Column 8 shows how the abundances change when solar abundances obtained using the HM model atmosphere are replaced by those given by the solar model by Bell et al. (1976). Values listed in this column provide a guess about uncertainties related to the structure of the model atmosphere.

Comparison of the values listed in Table 1 with those given in the analogous tables of Gratton & Sneden (1991, 1994) (where typical overall uncertainties of the element-to-iron abundance ratios were 0.05 – 0.08 dex) reveals that the abundances for the elements considered in this paper are often much more sensitive on uncertainties in the atmospheric parameters (due to different sensitivities on temperature and pressure) and in the structure of the model atmosphere (since lines form at various depths). In particular, the concentration of various molecules (like C_2 and CN) is very sensitive to temperature and pressure in the outer (and cooler) regions of the stellar atmospheres. On the other hand, O and C abundances deduced from high excitation, permitted lines are strongly sensitive to temperature in the deepest part of the atmospheres, and hence on how convection is handled when computing models. Finally, the abundance ratios are sensitive to the adopted values for the microturbulent velocities because thermal motions are larger than microturbulent velocities for these light species. The smaller overall sensitivity to uncertainties in the atmospheric parameters and model atmospheres of O and C abundances deduced from [OI] and CH lines support their use as primary abundance indicators.

3.1. Oxygen

The present oxygen abundances are based on the forbidden line at 6300.3 Å, which is considered a first class abundance indicator (Lambert 1978), and on the analysis of the high excitation, permitted triplets at 615.8 and 777 nm, including a complete treatment of the non-LTE effects on the abundances derived from this last two indicators (see Paper II for an exhaustive discussion about these statistical equilibrium calculations). However, since there is still no general agreement about non-LTE corrections, we listed also the abundances obtained from the LTE analysis. Oscillator strengths gf's were from Garstang (1976) for the forbidden line, and from Biémont et al. (1991) for the permitted ones. EWs for O lines in the 19 stars of our sample are listed in Table 2 (only available in electronic form).

O abundance determinations made (as in the present paper) using both permitted and forbidden lines ought to be more reliable than those using just one of these transitions. [O I] lines are weak in warm subdwarfs; on the other side, lines of the high excitation triplet are weak in cool giants. Analyses based on forbidden lines in metal-poor giants and on the IR triplets in subdwarfs probably introduce significant biases (see also Gratton 1990; 1993).

Table 2. Equivalent widths for O lines and Na lines in the 19 stars of our sample. Available only in electronic form

3.2. Carbon

Carbon abundances for the stars in our original data set were derived from a comparison of observed and synthetic spectra of the wavelength region 4207–4225 Å, which includes several features due to the R branch of the $A^2\Pi - X^2\Sigma$ ($\Delta v = 0$) transition of CH. For a few, generally metal-rich stars, additional information were provided by a similar comparison for the spectral feature at 5086 Å, mainly due to lines of the C_2 Swan system. Unfortunately, C_2 lines are vanishingly weak in most metal-poor stars. Both these sets of abundance indices were considered by Lambert (1978) in his analysis of the solar Carbon abundance: Lambert derived values of log n(C)=8.67 and 8.73 from the CH $A - X$ and the C_2 Swan bands respectively. While Lambert observed that the CH $A - X$ band cannot be considered the best abundance indicator in the Sun (due to concern in the correct location of the continuum level at these short wavelengths), it is the best choice in metal-poor stars, as shown by Sneden et al. (1986) and TLLS. In particular, TLLS showed that a systematic error is possibly present in their C abundances obtained from C I lines around 9100 Å: the derived abundances show a residual trend with $T_{\rm eff}$ that vanishes when the C abundance is instead obtained from CH (see their Fig. 8)[4].

The dissociation potential for CH has been determined with high accuracy at $D_o^o = 3.464$ eV (Brzozowski et al. 1976). Unfortunately, situation is not so good for the band oscillator strengths (see discussions in Grevesse & Sauval 1973 and Chmielewski 1984). Furthermore, predissociation greatly affects the strength of transitions with rotational quantum numbers R larger than $R \sim 20$ for the (0,0) band, $R \sim 10$ for the (1,1) band, and with any value of R for the (2,2) band. Hence, we prefer to use the band oscillator strengths deduced by Chmielewski (1984) from an analysis of the solar spectrum. The lines considered by Chmielewski have rotational quantum numbers similar to those considered here (actually the set of lines used in his study overlaps with our), and therefore use of his recommended values is appropriate here. Since the band oscillator strengths are taken from a solar analysis, it is not surprising that the synthetic spectra show good consistency with the KPNO solar flux spectrum (Kurucz et al. 1984).

The basic parameters for the synthesis of the C_2 feature at 5086 Å were taken from Lambert & Ries (1981). Again, a comparison with the solar flux spectrum yields a good agreement.

In the reanalysis of literature data, we considered only EWs for atomic lines, since spectral profiles required for compar-

[3] An error of ± 0.25 kms^{-1} in $v_{\rm t}$ was considered for giants, since for these stars $v_{\rm t}$ is very well constrained from our spectra

[4] We will later show that this trend is canceled when our $T_{\rm eff}$ scale is adopted

isons with synthesis of molecular features were not available. Three groups of features were considered: permitted high excitation lines close to 9100 (Clegg et al. 1981; TLLS) and 7100 Å (Tomkin et al. 1995), and the forbidden line at 8727 Å (Andersson & Edvardsson 1994). Features of the first group are stronger, and can be observed in very metal poor stars, while the others are weak and can only be observed in disk stars. In the analysis of these lines we used line data from the original papers: it should be noticed that the solar abundances obtained with the permitted lines near 7100 Å(log n(C)=8.66) and the forbidden line (log n(C)=8.67) agree very well with the recommended solar abundance of log n(C)=8.60 (Grevesse et al. 1991).

While the effects of departures from LTE are certainly negligible for the weak [CI] line, they might be more significant for the high excitation permitted line. Statistical equilibrium calculations for the C features considered in this paper have been carried out by Stürenburg & Holweger (1990) and Tomkin et al. (1992, 1995). These calculations indicate that non-LTE abundance corrections are small (< 0.1 dex) for the lines near 7100 Å (hence we simply adopted the LTE values). However, they may be not negligible for the stronger lines near 9100 Å, depending on the adopted cross sections for collisions with HI atoms (TLLS). To take into account these non-LTE effects, we corrected the average C abundances from the reanalysis of TLLS EWs by the same amount they did.

3.3. Nitrogen

We obtained nitrogen abundances using a number of CN features due to the $\Delta v = -1$ bands of the violet system ($B^2\Sigma - X^2\Sigma$) near the bandhead at 4215 Å [5], and the 2,0 vibrational band of the red system ($A^2\Pi - X^2\Sigma$) in the wavelength range 7910-7982 Å. Unluckily, no observation were available for the NH bands. The dissociation potential of CN is not well determined (see e.g. the discussions in Lambert 1978, and Lambert & Ries 1981), with values ranging from 7.5 to 7.9 eV: this is still the major source of uncertainty in the derived abundances of N from CN. In fact, the above mentioned range translates in a factor of about 3 in the derived N abundances. Here we will assume a value of $D_o^o = 7.65$ eV (Engleman & Rouse 1975). The f_{00} oscillator strength of the violet band was taken from Danylewych & Nicholls (1978), while the Franck-Condon factors were from Dwivedi et al. (1978). Band strengths of the red system are discussed in Sneden & Lambert (1982), who also compared theoretical values with those derived from analysis of the solar spectrum. Here we adopted their solar oscillator strengths for the (2,0) band, and verified that they well reproduce the KPNO solar flux spectrum.

3.4. $^{12}C/^{13}C$ ratio

The ^{12}C/^{13}C ratio was determined by a spectral synthesis of three ^{13}CH features at 4211.46, 4213.13, and 4221.83 Å, since most of the higher quality ^{13}CH indicators listed by Sneden et al. (1986) were not observed, and ^{12}C^{13}C and ^{13}CN lines are extremely weak in the spectra of the program stars. The positions of ^{13}CH lines were computed using the same code and molecular parameters considered by Sneden et al., while concentration was obtained using the same precepts adopted for ^{12}CH. Comparison of synthesized spectra with the solar one gives a good match for the canonical solar ^{12}C/^{13}C ratio of 89; however, this comparison is not so meaningful here, due to the large solar ^{12}C/^{13}C ratio. We may however compare the present ^{12}C/^{13}C ratios with those determined by Sneden et al. for 3 giants in common between the two samples: on average, our ^{12}C/^{13}C ratios are larger by 24 ± 14% (σ =25%). We attribute this difference to our use of not first class indicators; however, we will adopt our ^{12}C/^{13}C ratios with no further correction.

3.5. Sodium

Na abundances for stars in the original sample mainly rest on the EWs for the yellow doublet at 5682 and 5688 Å, for which we performed a full non-LTE analysis (see Paper II for details). However, since there is still no general agreement about non-LTE corrections, we listed also the abundances obtained from the LTE analysis. Additional information is provided by the line at 6154 Å (the other component of this doublet has not been observed), and by the weak line at 4751 Å (see Table 2). All these lines are listed as clean lines in the Holweger (1971) analysis of the photospheric Na abundance; the profile of the 5682.647 Å line shows actually some distortion in the short wavelength side in the solar spectrum, due to contamination by a weak, high excitation (E.P.=3.84 eV) Cr I line at 5682.493 Å. However, synthetic spectra for both the Sun and the program stars show that this contamination does not affect significatively the abundance derivation: the mean difference between abundances extracted from the 5682 and the (clean) 5688 Å line is only 0.04 ± 0.02 dex ($\sigma = 0.10$ dex). In Table 2 we listed the EWs measured for Na in the program stars. Data gathered from the literature include EWs for both the 5682-88 Å and 6154-60 Å doublets.

gfs for all sodium lines can be accurately computed (see e.g. Lambert & Warner 1968). Of more concern is the uncertain value of collisional damping parameters, since lines used in the present analysis are rather strong in metal-rich stars. Holweger (1971) obtained a rather large value of the enhancement factor for Na lines ($\log E = 0.8$) by ruling out any dependence of the abundances on line strength; we obtained a very similar value ($\log E = 0.73 \pm 0.14$) by repeating the same procedure with our code, the HM solar model atmosphere, and a depth independent microturbulent velocity of 0.9 kms^{-1} (Simmons & Blackwell 1982). The solar sodium abundance provided by the program lines is log n(Na)=6.31, identical to the meteoritic value (Anders & Grevesse 1989); however, for consistency with a forthcoming study of globular cluster giants (Carretta & Gratton 2000b), we adopted a solar value of log n(Na)=6.33, as derived from Anders & Grevesse (1989).

[5] The bandhead itself is severely blended with the strong resonance line of Sr II and cannot be used

Table 3. CNO abundances and $^{12}C/^{13}C$ ratios for the 19 program stars (available only in electronic form)

Table 4. Reanalysis of data by Tomkin et al. (1992): TLLS (available only in electronic form)

Table 5. Reanalysis of data by Sneden et al. (1991) and Kraft et al. (1992): SKPL(available only in electronic form)

Table 6. Reanalysis of data by Edvardsson et al. (1993): E93 (available only in electronic form)

Table 7. Reanalysis of data by Zhao & Magain (1990): ZM90 (available only in electronic form)

3.6. Magnesium

Our magnesium abundances are based on the red triplet at 6318–6319 Å, on the singlet line at 4730 Å, and on the intercombination line at 4571 Å. This last line is very clean in the solar spectrum, and it has been used by various authors as a diagnostic of the solar chromosphere (see e.g. Mauas et al. 1988); there has been however some confusion in the astronomical literature about its gf: e.g. Zhao & Magain (private communication) used a value of $\log gf = -5.44$, which yields a discrepant value for the solar Mg abundance. However, the $gf-$value for this line of $\log gf = -5.69$ has been determined from accurate lifetime measurements (Kwong et al. 1982): a solar analysis with this value of the gf, an EW of 101 mÅ (Steffen 1985) and the K92 solar atmosphere yielded a value of the abundance of Mg of log n(Mg)=7.65, in good agreement with that obtained from the other lines in our list (log n(Mg)=7.60 ± 0.02) and with the meteoritic Mg abundance of log n(Mg)=7.58 ± 0.02 (Anders & Grevesse 1989). The other lines employed in our analysis are listed as clean by Lambert & Luck (1978), and have accurate gf's (Froese-Fisher 1975a, 1975b; Mendoza & Zeippen 1987). However the red triplet is so close that it is not well resolved even on our rather high resolution spectra; and the 4730.038 Å line is blended with a Cr I line at 4729.859 Å, so that accurate $EW s$ are not easily derived for these features. We then adopted the abundances given by comparison with synthetic spectra. Reanalysis of literature data uses EWs both for the intercombination and high excitation Mg I lines.

4. Results

CNO abundances and $^{12}C/^{13}C$ for our program stars are listed in Table 3; Tables from 4 to 7 list the results from the reanalysis of literature data (TLLS, SKPL, E93 and ZM90, respectively). These tables are available only in electronic form.

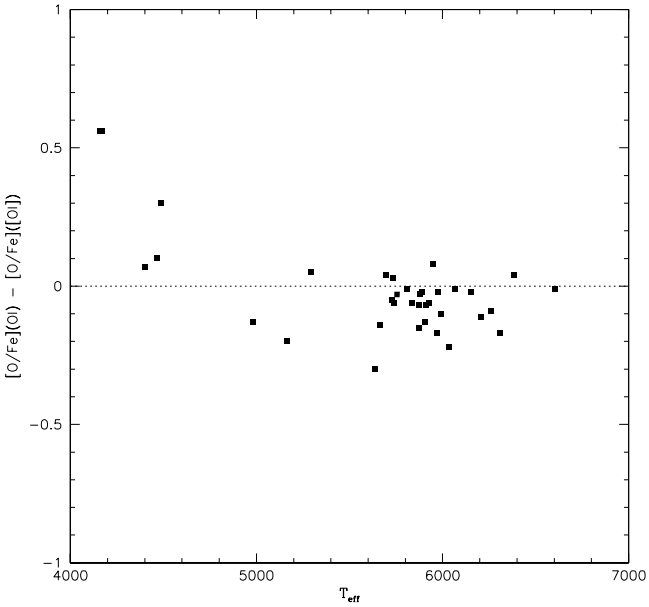

Fig. 1. Run of the [O/Fe] difference from permitted and forbidden lines against $T_{\rm eff}$

4.1. Oxygen

All our results for O include corrections for non-LTE effects obtained following the procedure described in Paper II, $i.e.$ including statistical equilibrium calculations based on empirically calibrated collisional H I cross sections.

Mean residual between O abundances deduced from permitted and forbidden lines is 0.01 ± 0.03 dex ($\sigma = 0.18$ dex; 40 stars). This difference is plotted against $T_{\rm eff}$ in Fig. 1.

As one can see, residuals for the coolest stars are much larger than average; this can be attributed to inadequacy of K92 models with the overshooting option switched on to describe the atmospheres of these cool stars (see Paper I and discussion below). Note that better agreement between different O diagnostics as well as a better equilibrium of ionization for Fe are obtained using the Kurucz models with no overshooting used in Gratton et al. (2000a); however, since these models became available to us only after all computations for the present paper were completed, and since abundances relative to the Sun obtained with the two sets of models agree very well each other for stars warmer than $T_{\rm eff}$ =4600 K, we decided not to repeat these lengthy computations and simply eliminated stars cooler than this limit from further discussion. Once this was done, the mean residual between O abundances provided by permitted and forbidden lines is -0.06 ± 0.02 dex (32 stars; $\sigma = 0.15$ dex); both mean difference and scatter are very small. Note that in our analysis we assumed a solar O abundance of log n(O)=8.93, the value recommended by Anders & Grevesse (1989) from an analysis of the forbidden lines and OH bands. However, a study of permitted lines in the Sun (Biémont et al. 1991) gives a solar O abundance of log n(O)=8.86; the difference with the abundance from forbidden lines found in the Sun is then almost the same we found in field stars.

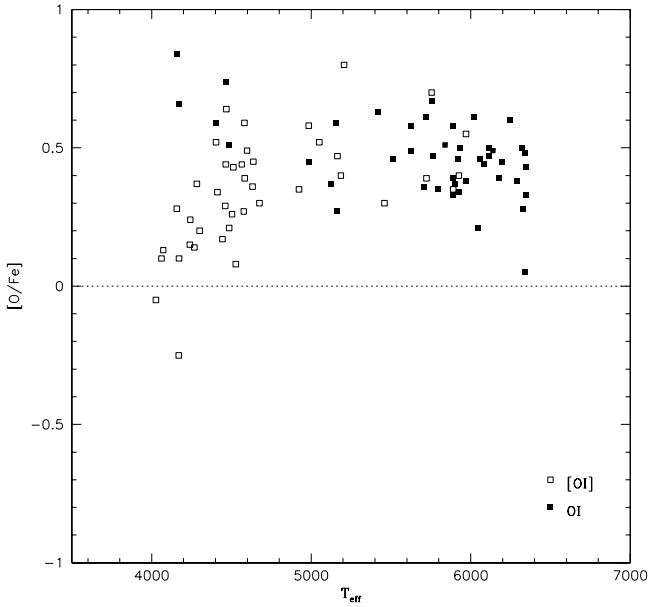

Fig. 2. Run of the [O/Fe] ratios with $T_{\rm eff}$ in metal-poor stars ([Fe/H]< -0.7. Different symbols are used for abundances derived from permitted (filled symbols) and forbidden lines (open symbols)

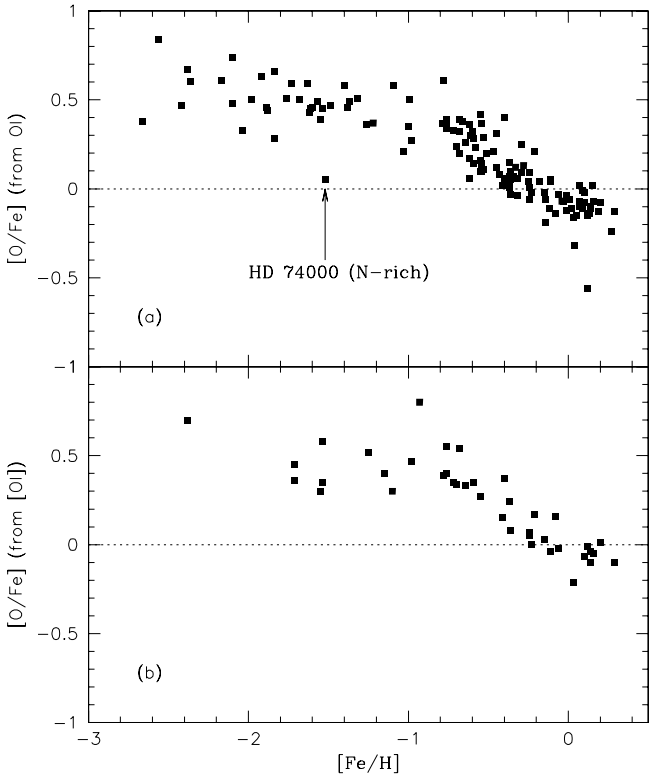

Fig. 3. Run of the [O/Fe] ratios vs [Fe/H] in metal-poor field stars. [O/Fe] ratios are obtained from permitted (panel a) and from forbidden (panel b) lines; only stars with $T_{\rm eff} > 4600$ K were considered. The N-rich dwarf HD 74000 is indicated, while the other N-rich dwarf present in our samples, HD 25329, has been omitted, since it has only an upper limit for O abundance

Of course, this result depends on the adopted non-LTE corrections, which stem from our own statistical equilibrium calculations. However, we found that these corrections are small: on average, abundances derived from IR permitted lines must be lowered by 0.06 dex, the largest correction ($\sim$ 0.25 dex) being obtained for the warmest stars. Explorative computations with x=0.03 and x=3 (the extreme values of the multiplicative factor x for H I collisions compatible with observations of RR Lyrae; see Paper II for the definition of x) show that the non-LTE corrections are uncertain by about ± 0.1 dex for these stars.

Fig. 2 shows the run of the [O/Fe] ratio with $T_{\rm eff}$ for stars with [Fe/H]< -0.7, both from permitted and forbidden lines. Systematic trends in abundances derived from both indicators are clearly present. These trends cannot be attributed to an evolutionary effect for two reasons:

1. Permitted and forbidden lines exhibit opposite trends
2. Three of the stars in the SKPL sample are likely to be in evolutionary phases later than the RGB, according to their position in the $(b-y)-c_1$ diagram of Twarog & Anthony-Twarog (1994): two of them are probably horizontal branch stars (BD+11^{0}2998: [O/Fe]=+0.30; and HD 166161: [O/Fe]=+0.40), while the third one is likely to be at the base of the asymptotic giant branch (HD 204543: [O/Fe]=+0.36). Their [O/Fe] ratios are much larger than those measured in several cooler stars, and actually do not differ significantly from the average obtained for warm stars.

Departures from LTE are not expected for the forbidden lines. Hence, the most likely explanation for the trend with $T_{\rm eff}$ is large deviations of the atmospheric structure from that of K92 models used in this paper, that seem to be not fully adequate to reproduce the coolest stars. This last possibility is also supported by the poor equilibrium of ionization we get for Fe (Paper I).

It seems then safer to consider only warm stars when examining the run of the [O/Fe] ratio with [Fe/H]. Panels a and b of Fig. 3 display the run of the [O/Fe] ratio against overall metal abundance [Fe/H] for permitted and forbidden lines respectively; only stars with $T_{\rm eff} > 4600$ K were considered. The two runs appear to be very similar; while a small upward trend in [O/Fe] among the most metal-poor stars may exist (somewhat in agreement with the recent results based on the OH band by Israelian et al. 1998, and Boesgaard et al. 1999, although less pronounced than found by these authors), we will hereinafter adopt an average value for the O overabundance in all metal-poor stars. This average value (from forbidden lines) in warm metal-poor stars is:

$$[{\rm O/Fe}] = +0.48 \pm 0.05 \ {\rm dex} \quad (\sigma = 0.16 \ {\rm dex}, \ 11 \ {\rm stars}),$$

which is indeed very close to the value obtained from permitted lines:

$$[{\rm O/Fe}] = +0.45 \pm 0.02 \ {\rm dex} \quad (\sigma = 0.13 \ {\rm dex}, \ 33 \ {\rm stars}),$$

This agreement is due to the adoption of a $T_{\rm eff}$'s scale about 100–150 K higher than the ones (e.g. Carney 1983; Magain 1987) used in previous abundance analysis of subdwarfs (see

also Paper I). Note that in no case we obtain [O/Fe]> 1; hence we cannot confirm the large O overabundances found by Abia & Rebolo (1989) for the most metal metal-poor stars. On the basis of our results and of various discussions in the literature (e.g. TLLS) we confirm that their overestimates are mainly due to errors in the EWs and to the adoption of Carney (1983) $T_{\rm eff}$'s scale (see also King 1993). The use of a linear run of [O/Fe] vs [Fe/H], with no $plateau$ at low metallicity should be strictly avoided when interpreting the colour-magnitude diagrams of globular clusters, in order to obtain reliable distances and ages (see Buonanno et al. 1989 for a discussion of this point).

From our results, we conclude that O abundances derived from permitted and forbidden lines are in good agreement each other, for stars with $T_{\rm eff} > 4600$ K and in the following we will adopt the average abundances. The mean overabundance of O in field stars, derived both from permitted and forbidden lines, is then:

$$[\mathrm{O/Fe}] = +0.46 \pm 0.02 \,\mathrm{dex} \quad (\sigma = 0.12 \,\mathrm{dex},\ 32 \,\mathrm{stars}),$$

This mean overabundance also agrees with other recent estimates: [O/Fe]=0.41 from the forbidden lines in the spectra of giants (Sneden et al. 1991); and [O/Fe]=0.52 from the permitted lines in the spectra of dwarfs (King 1993).

4.2. Carbon

Carbon abundances provided by CH and C_2 lines for our original star list are listed in Columns 3 and 4 of Table 3 respectively. Abundances from the C_2 blend at 5086 Å are available only for 6 metal rich dwarfs; on average, they are slightly larger than those given by the CH lines in the range 4203–4224 Å by 0.08 ± 0.02 dex (the r.m.s. scatter is 0.05 dex). This systematic difference is small, although it seems to be significant[6]. However, the large differences between the C abundances obtained using C_2 lines when different solar model atmospheres are considered (see Table 1) might suggest that the structure of the model atmospheres plays an important rôle here. Luckily, [C/Fe] ratios deduced from CH lines are much less sensitive on the adopted model atmospheres: hence, they will be considered in the following discussion.

Carbon abundances from atomic lines for the reanalyzed samples are listed in Table 4 (data for the TLLS sample) and 6 (those for the E93, obtained using both permitted and forbidden lines: see Clegg et al. 1981; Tomkin et al. 1995; and Andersson & Edvardsson 1994). For 12 stars we have data both from low excitation forbidden and high excitation permitted lines: abundances from permitted lines are on average larger by 0.03 ± 0.05 dex ($\sigma = 0.19$ dex). The mean difference is very small, but there might be a small trend for increasing differences with decreasing $T_{\rm eff}$. A larger sample is required to explore this issue.

[6] In the analysis of Lambert (1978) of the solar C abundance, the difference between the values obtained from the same transition considered here ranges from 0.06 to 0.15 dex, depending on the model atmosphere used. The HM model gives a difference of 0.09 dex, in agreement with the value we found within observational errors.

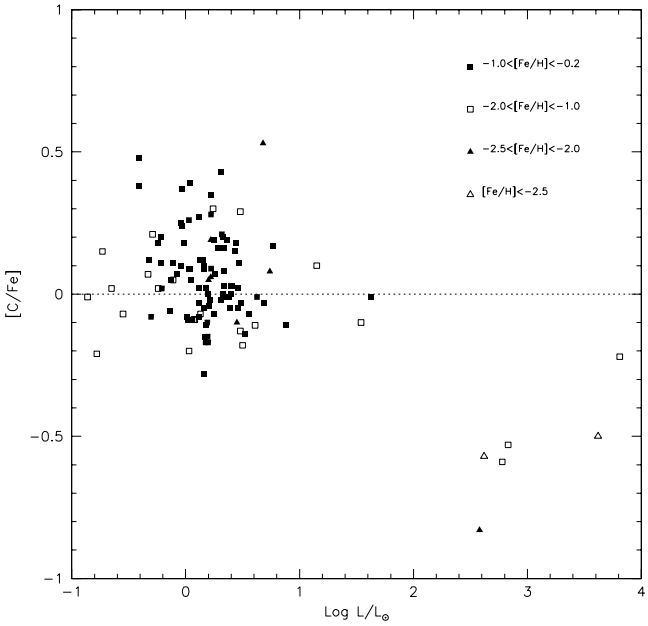

Fig. 4. Run of the [C/Fe] ratio against stellar luminosity for the stars analyzed in the present paper. Different symbols represent stars in different bins of metal abundance

Before discussing the run of C abundances with overall metallicity, stars which have undergone mixing episodes must be eliminated, since C is expected to be depleted in luminous giants (see Fig. 4, where we used different symbols for stars in different bins of metal abundances). However, the precise location of the first dredge up cannot be determined from these data alone, due the lack of stars of intermediate luminosities ($1 < \log L/\,L_{\odot} < 2.5$). This issue is considered in detail in another analysis (Gratton et al. 2000a). In Fig. 5 we have plotted [C/Fe] ratios determined from the G-band in the present work and from a compilation of literature studies. While the scatter of these [C/Fe] ratios is large (data include C abundances determined from low dispersion spectra as well as higher quality determinations), this figure reveals that the depletion of surface C abundances occurs at a luminosity around $\log L/\,L_{\odot} \sim 2$, or slightly fainter, in agreement with predictions from evolutionary models (Sneden et al. 1986), and with observations of stars in metal-poor globular clusters (see e.g. Bell et al. 1990), and with the results of Gratton et al. (2000a). Since there is no evidence that any appreciable C depletion has occurred for stars as bright as $\log L/\,L_{\odot} \sim 1.5$, in the following we will assume that stars fainter than this limit have the original surface C abundance.

We may now plot in Fig. 6 the run of the [C/Fe] ratio with [Fe/H] for *bona fide* unmixed stars (i.e. those with $\log L/\,L_{\odot} < 1.5$). Fig. 6 shows that the [C/Fe] ratio is roughly solar over the whole metallicity regime explored in this paper. The moderate overabundances in the most metal-poor disk stars suggested by Andersson & Edvardsson (1994) and Tomkin et al. (1995) are reduced to a marginally significant ~ 0.1 dex value in our reanalysis of their data: this is mainly due to the adoption of a higher $T_{\rm eff}$ scale. We finally warn the reader that the [C/Fe] run of Fig. 6 is obtained by combining data provided by the

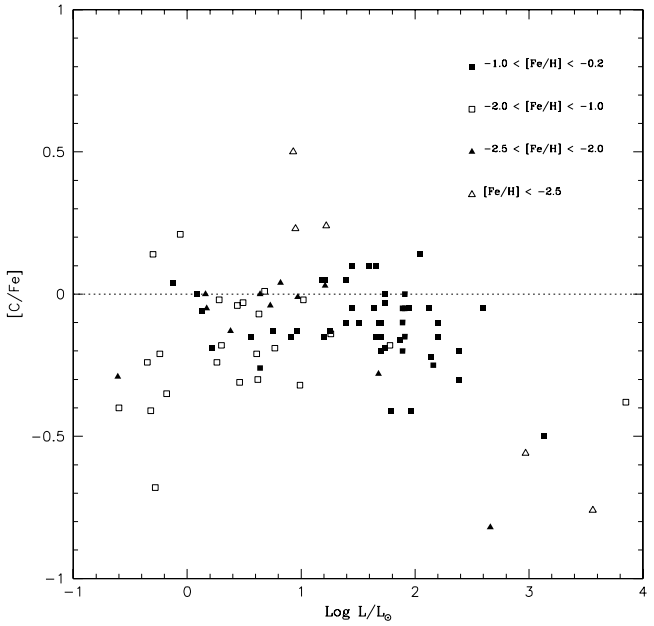

Fig. 5. Run of the [C/Fe] ratio against stellar luminosity in metal-poor stars ([Fe/H]< -0.2) from a compilation of selected studies (Cottrell & Sneden 1986; Luck 1991; this paper). Different symbols represent stars in different bins of metal abundance

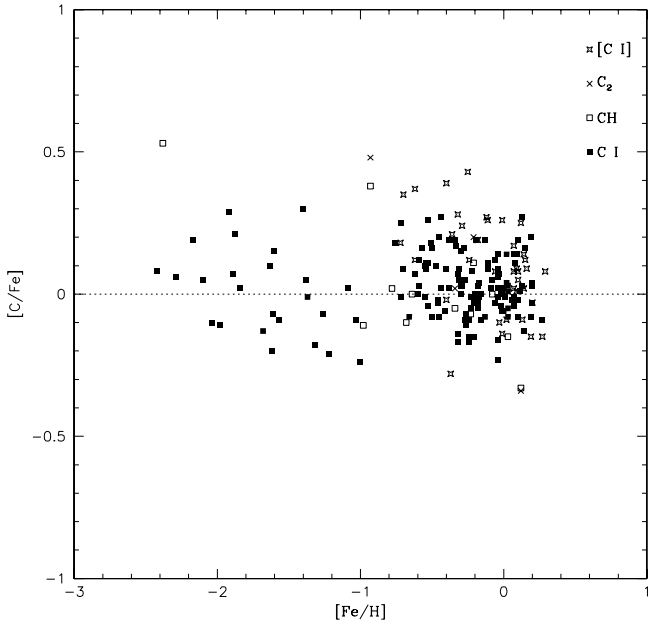

Fig. 6. Run of the [C/Fe] ratio against [Fe/H] in unmixed stars ($\log L/\,L_{\odot} < 1.5$). Different symbols are used for C abundances obtained from different indices

analysis of various features; while the overall trend seem well defined (different indices yielding similar results), small offsets might still be present. A more comprehensive study overcoming the selection biases present in all available samples would be welcome.

4.3. $^{12}C/^{13}C$

Panels a and b of Fig. 7 display the run of the ^{12}C/^{13}C ratio against stellar luminosity for stars with -0.9 <[Fe/H]< -0.2, and for stars with [Fe/H]< -0.9 respectively.

Plotted data include ^{12}C/^{13}C ratios determined in this paper, as well as those by Sneden et al. (1986) and Shetrone et al. (1993). Both panels indicate that the ^{12}C/^{13}C ratio declines with increasing luminosity: in fact, stars with $\log L/\,L_{\odot} < 1.5$ have very large values of the ^{12}C/^{13}C ratios (in most cases, only lower limits can be determined), while very small values (4–10) have been obtained for stars with $\log L/\,L_{\odot} > 2$. These data confirm earlier findings for both field and cluster stars (see e.g. Gilroy & Brown 1991; and Gratton et al. 2000a), and the lack of evidences for mixing in stars with $\log L/\,L_{\odot} < 1.5$.

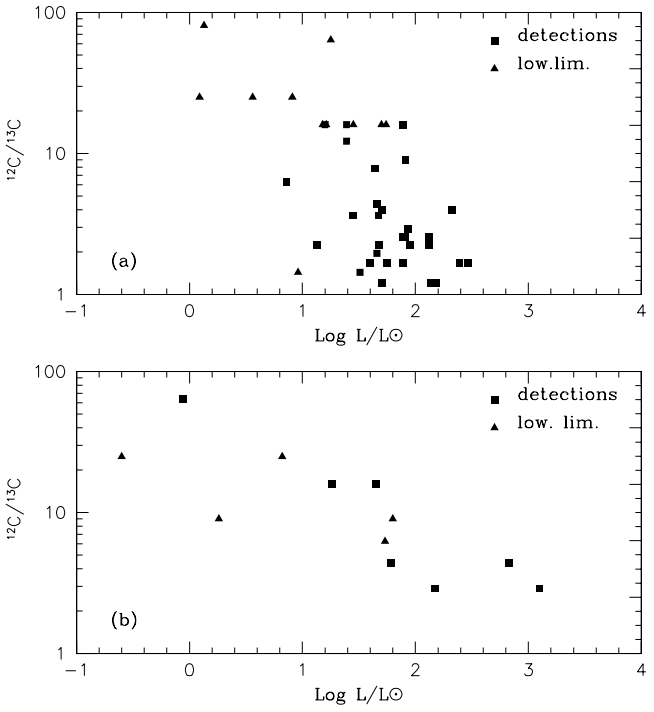

Fig. 7a and b. Run of the ^{12}C/^{13}C ratio against stellar luminosity for stars with -0.9 <[Fe/H]< -0.2 (panel **a**), and for stars with [Fe/H]$<$ -0.9 (panel **b**). Plotted data includes ^{12}C/^{13}C ratios determined in this paper, as well as those by Sneden et al. (1986) and Shetrone et al. (1993). Rectangles represent actual detections, while triangles represent lower limits

4.4. Nitrogen

N abundances are listed in Columns 5, 6 and 7 of Table 3; they were obtained only for stars in our original sample. In some spectra, CN features are very weak, and only upper limits can be obtained. Furthermore, there might be a systematic offset in our nitrogen abundances, due both to errors in the C abundances and to uncertainties in the same analysis of CN (e.g. related to uncertainties in the dissociation potential for this molecule). Conclusions are thus not as clean as those obtained for the other elements. The comparison between abundances provided by lines due to 4 blends of the blue system (between 4211 and

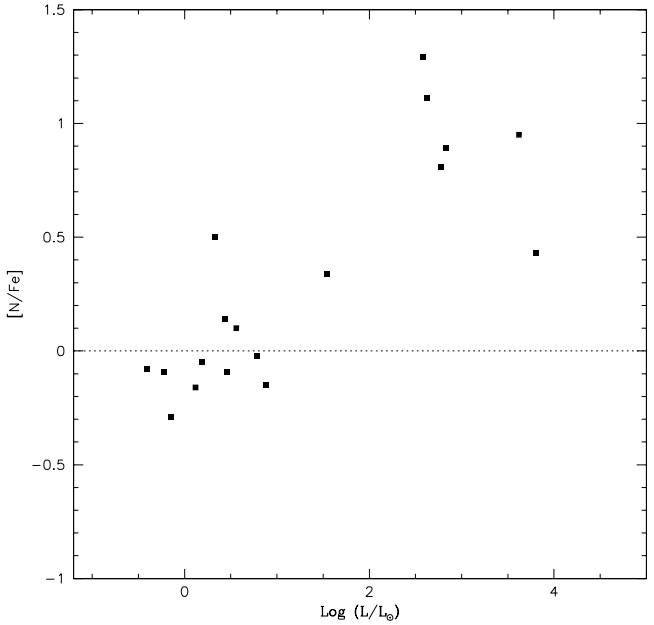

Fig. 8. Run of the [N/Fe] ratios against stellar luminosity for our program stars

Table 8. Na abundances in the 19 program stars (available only in electronic form)

4216 Å) and about 40 blends of the red system (between 7912 and 7980 Å) is rather good. On average, N abundances given by the blue system are larger by 0.12 ± 0.07 dex ($\sigma = 0.19$ dex, 8 stars). A large part of this difference is due to a single star (HD 136316) having very weak lines of the red system; once this star is dropped, the average difference is 0.07 ± 0.04 dex ($\sigma = 0.12$ dex, 7 stars), which may be attributed to small errors in the location of the continuum level in our line crowded, blue spectra. In the following, we simply averaged the N abundances provided by the two systems.

The run of the [N/Fe] ratio against stellar luminosity is shown in Fig. 8. There is an obvious trend for increasing N abundances with increasing luminosity which is clearly symmetric with respect to the run of the [C/Fe] ratio: stars with $\log L/\,L_{\odot} < 2$ have [N/Fe]=$+0.02 \pm 0.07$ dex ($\sigma = 0.22$ dex, 11 stars), while more luminous stars have [N/Fe]=$+0.91 \pm 0.11$ dex ($\sigma = 0.27$ dex, 6 stars). As well known, this is exactly what expected if N-rich, C-poor material is brought to the surface from regions of CNO-cycle H-burning.

Mean [(C+N)/Fe] ratios (Table 3) for stars fainter and brighter than $\log L/\,L_{\odot} = 2$ are 0.03 ± 0.05 dex ($\sigma = 0.17$ dex, 13 stars) and 0.32 ± 0.08 dex ($\sigma = 0.19$ dex, 6 stars) respectively. However, we are not inclined to give much weight to this difference, due to possible systematic errors in abundances deduced from molecular species related to the uncertain values of the dissociation energy. Moreover, in our sample, the most luminous stars are also more metal-poor: hence, the systematic trend of the [(C+N)/Fe] ratio with luminosity might be due to a trend with metal abundance.

Unluckily, our sample cannot be used to constrain the run of the [N/Fe] ratio with metal abundance, since N abundances were obtained only for metal-rich stars or stars in which mixing events have already changed the original abundances.

4.5. Sodium

Non-LTE corrections for the Na lines considered in the present work are rather small (< 0.08 dex) both for the Sun and for moderately metal-poor dwarfs (in these last cases they are slightly positive: ~ 0.03 dex). However, since corrections depend on stellar gravity, they are not negligible (up to 0.3 dex) for metal-poor giants. Moreover, corrections for these stars depend on the adopted value for the collisional cross-section (see also Paper II for a detailed discussion). In order to quantify this dependence, we repeated our statistical equilibrium computations for a typical metal-poor giant (HD 122956), using different values for the multiplicative constant x for the collisional cross-sections: x =0.001, 0.01 and 0.1. As expected, non-LTE corrections are negligible for large x values, but they are rather large (about 0.4 dex) for x=0.001. This last value yields cross sections much smaller than those estimated by Kaulakys (1985, 1986), but it is however still compatible with RR Lyrae observations (see also Paper II).

Table 8 (available only in electronic form) lists sodium abundances (with and without non-LTE corrections), along with the EWs of individual lines for the stars we observed directly. The average [Na/Fe] ratio for stars with [Fe/H]< -0.6 is -0.09 ± 0.05 ($\sigma = 0.19$, 13 stars). The scatter decreases if we omit the two coolest stars: in this case, the average is -0.04 ± 0.04 ($\sigma = 0.13$, 11 stars). The agreement obtained from different lines is excellent ($\sigma = 0.08$ dex).

Fig. 9 displays the run of the [Na/Fe] ratio with overall metal abundance for all stars considered in this paper; sodium abundances scale approximately as iron ones, being possibly overdeficient in stars with [Fe/H]~ -1. The scatter is larger than expected from the line-to-line comparison; it may be due to uncertainties in the atmospheric parameters, which might induce rather large errors in the [Na/Fe] ratios. However, part of this scatter might be real, since sodium is known to be overabundant in some globular cluster giants (see Kraft et al. 1992; Carretta & Gratton 2000b).

4.6. Magnesium

Barbuy et al. (1985) and Magain (1989) suggested that large discrepancies exist between abundances provided by the resonance intercombination line and higher excitation Mg lines in the spectra of red giants and subdwarfs. Magain estimated differences as large as 0.6 dex, apparently a strong function of surface gravity; he suggested that the dominant non-LTE effect for Mg should be overionization, and that the resonance line may require larger non-LTE corrections since there is a larger contribution in its formation from the outer atmospheric layers than in the case of the higher excitation lines. However, other studies obtained a much better agreement between abundances

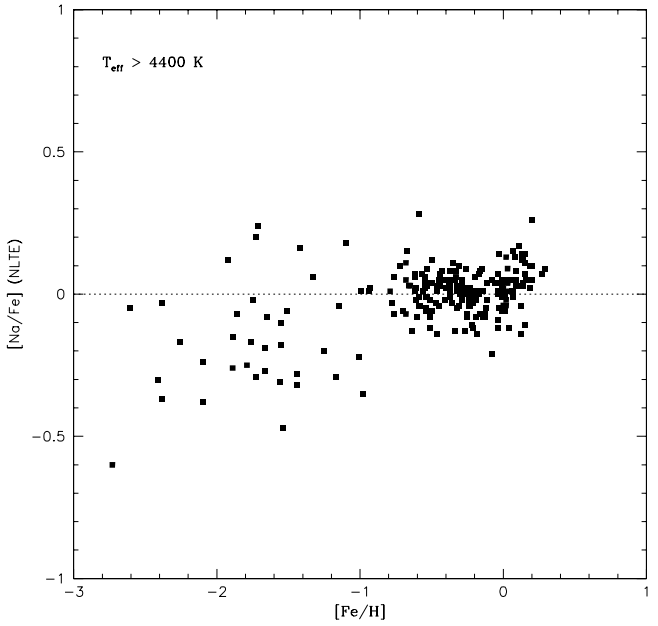

Fig. 9. Run of the [Na/Fe] ratio against overall metal abundance [Fe/H] for the stars of the total sample analyzed in the present paper

provided by different Mg lines: in an analysis of the spectra of RR Lyrae variables (Clementini et al. 1995), it was found that the Mg abundances deduced from the intercombination resonance line at 4571 Å are larger than those provided by higher excitation lines by 0.09 ± 0.08 dex; a similar result has been obtained in the present analysis for field, not-variable stars (in this case the mean difference is 0.06 ± 0.05 dex). This is due both to the different value for the gf of the intercombination line (see Sect. 3.6), and to the adoption of a higher $T_{\rm eff}$ -scale; however, to better clarify this issue we decided to perform detailed statistical equilibrium computations for a Mg I model atom (see Paper II for details).

The results of our non-LTE analysis for Mg are listed in Table 9 (available only in electronic form) for the 19 stars of the original sample; both the abundances given by individual features and the mean Mg values are indicated. The line-to-line scatter is moderately large ($\sigma = 0.13$ dex), due to the rather large range in excitation potential and line strength. The Mg to Fe ratio is moreover rather sensitive on the adopted values for the effective temperature and microturbulent velocity. On the whole, derived abundances are very similar to those (not shown here) obtained under LTE assumption: corrections are < 0.02 dex for the observed high excitation lines, that form at large optical depth and are usually very weak. Very small non-LTE corrections are found even for the intercombination line; they are in the range 0.05–0.10 dex only for cool and moderately metal-poor giants (HD 136316 and HD 187111). In these stars this line is very strong and heavily saturated.

In order to check the sensitivity of our statistical equilibrium computations to the value of the parameter x, the non-LTE abundance analysis has been repeated for the star having the largest corrections ($i.e.$ HD 187111). For this purpose, we used

Table 9. Magnesium abundances in the 19 program stars (available only in electronic form)

x =7, at the lower edge of the fiducial range as deduced from the observation of RR Lyrae stars (Paper II). As expected, our results show that Mg abundances are about 0.05 dex larger for all lines. We can then conclude that upper limits to non-LTE corrections for Mg abundances are 0.15 dex for the intercombination line and 0.10 dex for the other lines, in the stars of our program sample. The low Mg abundances obtained by Barbuy et al. (1985) and Magain (1989) when using the 4571 Å line cannot be explained as due to departures from LTE, and must be rather attributed to choice of the oscillator strength.

The [Mg/Fe] ratios of our program star sample seem to follow without discontinuity the run with overall metal abundance [Fe/H] obtained from the reanalysis of the E93 sample (listed in Table 6). However, some discrepancy is present in the abundances obtained from the reanalysis of the ZM90 sample (see Table 7). In this case [Mg/Fe] ratios derived from the intercombination line well agree with those obtained for our 19 program stars: mean values for stars with [Fe/H]< -0.6 are $+0.40 \pm 0.04$ dex and $+0.38 \pm 0.04$ dex respectively, once the appropriate corrections for deviations from LTE (that are little, anyway) are applied. On the other side, [Mg/Fe] ratios derived from high excitation lines are lower than those obtained for our sample: 0.27 ± 0.03 as compared to 0.38 ± 0.04.

Fig. 10 displays the run of the [Mg/Fe] ratio with overall metal abundance [Fe/H] from the intercombination line and the higher excitation lines. The reason of this discrepancy is not completely clear; we examined different hypoteses, like systematic differences in the oscillator strengths, in EWs and in adopted values of the microturbulent velocity. Our conclusion is that none of these causes can explain the observed difference. More promising is the possibility that departures from LTE (computed for the ZM90 sample with the x parameter recommended from the analysis of RR Lyrae stars) could be underestimated. In fact, corrections derived from the high excitation lines are larger for the warmest and most metal-poor stars, as the stars in the ZM90 sample are: while corrections for the intercombination line are larger in the coolest metal-poor stars.

Notwithstanding this (small) discrepancy, in the discussion of Paper IV we will consider the mean values of [Mg/Fe] obtained using all lines.

5. Comparisons with other recent abundance determinations

5.1. Boesgaard et al. 1999

Very recently, Boesgaard et al. (1999) published an analysis of the O abundances from OH lines, and reanalyzed literature data concerning OI (including some of the same data here considered, that is TLLS). Boesgaard et al. gave two different sets of abundances, derived using model atmospheres which used two

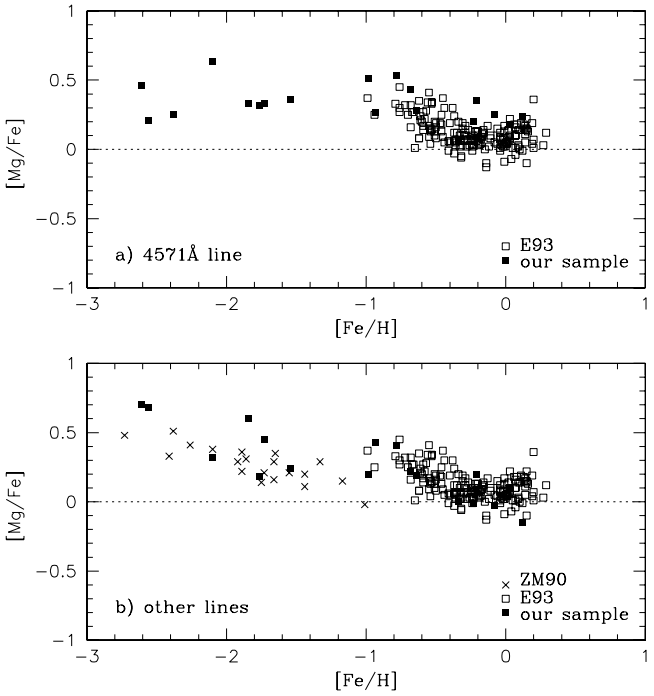

Fig. 10a and b. Run of the [Mg/Fe] ratio against overall metal abundance [Fe/H]. In panel **a** are plotted results from the intercombination line at 4571 Å and in panel **b** those derived from higher excitation lines, for all the stars in our total combined sample

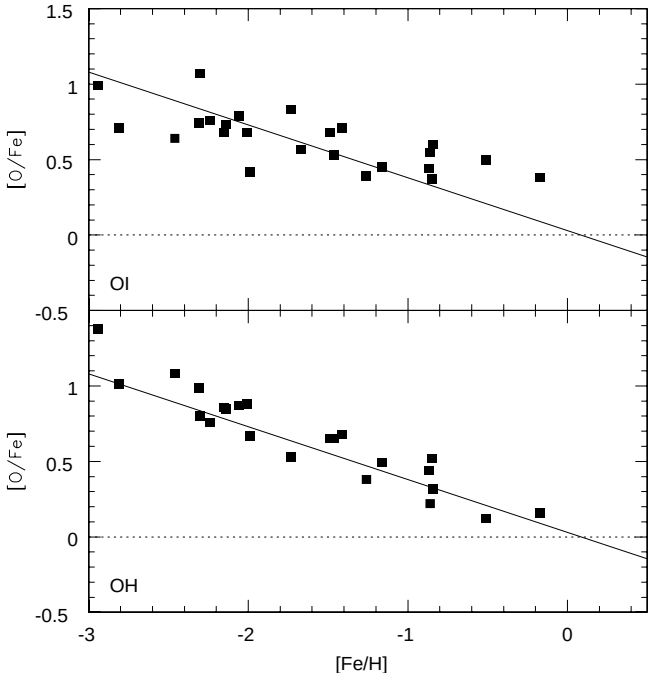

Fig. 11. Run of the [O/Fe] ratio with [Fe/H] determined by Boesgaard et al. (1999) using OI lines (upper panel) and the UV OH band (lower panel). Overimposed is the mean relation [O/Fe]=-0.35 (±0.03) [Fe/H] +0.03 (±0.05) proposed by Boesgaard et al.

different temperature scales. The highest one (labeled "King") agrees very well with the present one: for 20 stars in common, the mean difference is only 6 ± 15 K, with a scatter of 65 K for individual stars. Gravities are derived by averaging values from ionization equilibrium (the technique used in this paper) with those given by a calibration of Strömgren photometry. These gravities also compare very well with ours, the mean difference being 0.14 ± 0.03 dex, with a scatter for each star of 0.27 dex. Finally, their microturbulent velocities are on average 0.45 ± 0.08 km s^{-1} larger than ours: these larger values of the microturbulent velocity explain about half the average difference in the [Fe/H]'s (their values being smaller than ours on average by 0.09 ± 0.02 dex). Boesgaard et al. O abundances from permitted atomic lines are on average larger than ours by 0.09 ± 0.03 dex (scatter 0.13 dex), a difference that may be attributed to our adopted corrections for departures from LTE (these corrections are not included in the Boesgaard et al.'s O abundances). While we regard these differences as minor, we note that combining the higher O abundances with the lower [Fe/H]'s, on average the [O/Fe] values of Boesgaard et al. are higher than ours by 0.18 dex.

Since the present analysis reproduces quite well the results by Boesgaard et al., apart from small offsets in [Fe/H] and [O/Fe] that may be easily explained, it seems quite odd that our Fig. 3 does not support well their mean relation [O/Fe]=-0.35 (±0.03) [Fe/H] +0.03 (±0.05) (a similar steep slope was previously obtained by Israelian et al. 1998, still from analysis of OH bands in the extreme ground-based UV). Rather, our O abundances suggest a mild slope (~ -0.1) in the [O/Fe] ratios for stars with [Fe/H]< -1, with a rather abrupt change in the range $-1 <$[Fe/H]< -0.5, and then an almost constant value for higher metallicities (in Paper IV we will interprete such a relation within the framework of galactic evolution). Part of this difference may be attributed simply to statistics: we considered a much larger number of stars, mainly in the critical metal abundance range $-1 <$[Fe/H]< -0.5, corresponding to the transition from thick to thin disk. However, we note that the constant slope of the run of average [O/Fe] vs [Fe/H] found by Boesgaard et al. is due to their O abundances from OH, and not to those from OI lines. To show this, we plotted in Fig. 11 the runs of the [O/Fe] values with [Fe/H] obtained by Boesgaard et al. with O abundances from OI lines and from OH. Overimposed is the Boesgaard et al. mean relation: while this provides an excellent fit to the abundances from OH, the slope suggested by OI lines is much milder, and roughly in agreement with the impression given by our Fig. 3. While the issue of O abundance determinations is clearly not yet definitely settled, we argue that abundances from OH for stars in the metal abundance range $-1 <$[Fe/H]< -0.5 may be regarded with suspicion, since location of the continuum level is difficult at these wavelengths in such line rich spectra.

5.2. Gratton et al. 2000a

We are now publishing a separate paper on mixing episodes along the RGB (Gratton et al. 2000a). The two analysis are al-

most completely independent each other, using different observational material, a different set of atmospheric parameters, different line lists, and even slightly different model atmospheres (those used here are the Kurucz models with the overshooting option switched on; the paper on mixing uses the model atmospheres with the overshooting option switched off). However, there are 5 stars in common between the two samples (here we only considered stars in the original samples); they are all giants, with somewhat uncertain reddening estimates. On average adopted atmospheric parameters are quite similar, although with a quite large star-to-star scatter: present $T_{\rm eff}$'s and gravities are lower by 73 ± 73 K ($\sigma = 164$ K), and 0.19 ± 0.33 dex ($\sigma = 0.74$ dex), respectively. Average abundances are also quite similar: differences (in the sense this paper-Gratton et al. 2000a) are are -0.03 ± 0.09, 0.13 ± 0.07, 0.00 ± 0.08, and -0.10 ± 0.23 dex for [Fe/H], [C/Fe] (from CH), and [O/Fe] (from [OI] and OI lines), respectively. Scatter for individual stars is however quite large (0.21, 0.15, 0.17, and 0.33 dex). These slightly different results are due to the different choice about the atmospheric parameters. If we would adopt the same parameters for these stars used in Gratton et al. (2000a), we would have obtained average differences of 0.07 ± 0.02, 0.03 ± 0.06, 0.06 ± 0.04, and -0.03 ± 0.02 dex for [Fe/H], [C/Fe] (from CH), and [O/Fe] (from [OI] and OI lines), respectively, with much smaller scatter individual stars (0.05, 0.14, 0.10, and 0.03 dex). Finally, for Na we compared the abundances of this paper with those for the extended sample of Gratton et al. (2000a): from 21 stars, we get an average offset of 0.01 ± 0.05 dex ($\sigma = 0.22$ dex).

5.3. Fuhrmann 1998

A further interesting comparison is with the very precise recent analysis of nearby dwarfs and subgiants by Fuhrmann (1998). There are 32 stars in common between our paper and that of Fuhrmann. The agreement is very good: on average, our [Fe/H] are smaller by 0.02 ± 0.01 dex ($\sigma = 0.08$ dex), while the [Mg/Fe] values are larger by 0.01 ± 0.02 dex ($\sigma = 0.10$ dex). In Paper IV, when we will discuss the implications of the present data for galactic evolution, we will see that the conclusions we reach are very similar to those of Fuhrmann.

6. Conclusions

In this paper we have presented an analysis of the abundances of Fe, C, N, O, Na, and Mg in a large sample (~ 300) of field stars. Original data consisted in a new set of high resolution, high S/N spectra for 19 stars; these were complemented with high quality EWs from selected literature surveys. Whenever possible, we tried to compare results obtained with several abundance indices.

The main conclusions are:

1. Once the (small) corrections for non-LTE effects (presented in Gratton et al. 2000a: Paper II) are considered, O abundances derived from the permitted lines are fully consistent with those obtained using the forbidden line at 6300.3 Å for stars with $T_{\rm eff}$ >4600 K; this result agrees with that obtained by King (1993), but not with other studies using a lower $T_{\rm eff}$ -scale for subdwarfs. The O overabundance in metal-poor stars ([Fe/H]< -0.8) are 0.48 ± 0.05 dex ($\sigma = 0.16$ dex, 11 stars) and 0.45 ± 0.02 dex ($\sigma = 0.13$ dex, 33 stars) from forbidden and permitted lines respectively; the mean value is 0.46 ± 0.02 dex ($\sigma = 0.12$, 32 stars). However, the most luminous metal-poor field stars yield slightly smaller O abundances than fainter stars of similar metallicities. This is attributed to inadequacy of Kurucz (1992) model atmospheres with overshooting for stars cooler than ~ 4600 K. Our data suggest a general overabundance of O in metal-poor stars ([Fe/H]< -1), with only a gentle trend for decreasing O excesses with increasing metal abundances; these results are not well fitted by a constant slope in the relation between [O/Fe] and [Fe/H] recently suggested from the analysis of OH lines.
2. If only *bonafide* unmixed stars are considered, C abundances scale as Fe ones over the whole range explored ([Fe/H]< -2.5). We did not confirm the moderate C excess found by Andersson & Edvardsson (1994) and Tomkin et al. (1995) in metal-poor disk stars ($-0.8 <$[Fe/H]< -0.4); this is due to our adoption of a higher $T_{\rm eff}$ scale.
3. Na abundances scale as Fe ones in the high metallicity regime, while metal-poor stars present a Na underabundance. None of the field stars analyzed here belong to the group of O-poor and Na-rich stars observed in globular clusters.

In future papers of this series we will discuss these results in the framework of galactic chemical evolution.

References

Abia C., Rebolo R., 1989, ApJ 347, 186
Anders E., Grevesse N., 1989, Geochim. Cosmochim. Acta 53, 197
Andersson H., Edvardsson B., 1994, A&A 290, 590
Arnett W.D., 1973, ARA&A 11, 73
Balachandran S.C., Bell R.A., 1997, A&AS, 191, 7408
Balachandran S.C., Carney B.W., 1996, AJ 111, 946
Barbuy B., 1988, A&A 191, 121
Barbuy B., Erdelyi-Mendes M., 1989, A&A 214, 239
Barbuy B., Spite F., Spite M., 1985, A&AS 144, 343
Baschek B., Scholz M., Sedlmayr E., 1977, A&A 55, 375
Bell R.A., Eriksson K., Gustafsson B., Nordlund A., 1976, A&AS 23, 37
Bell R.A., Briley M.M., Smith G.H., 1990, AJ 100, 187
Bessell M.S., Sutherland R.S., Ruan K., 1991, ApJ 383, L71
Biémont E., Hibbert A., Godefroid M., Vaek N., Fawcett B.C., 1991, ApJ 375, 818
Boesgaard A.M., King J.B., Deliyannis C.P., Vogt S., 1999, AJ 117, 492
Brzozowski J., Bunker P., Elander N., Erman P., 1976, ApJ 207, 414
Buonanno R., Corsi C.E., Fusi Pecci F., 1989, A&A 216, 80
Carbon D.F., Barbuy B., Kraft R.P., Friel E.D., Suntzeff N.B. 1987, PASP 99, 335
Carney B.W., 1983, AJ 88, 623
Carretta E., Gratton R.G., 2000a, in preparation (Paper V)
Carretta E., Gratton R.G., 2000b, in preparation

Castelli F., Gratton R.G., Kurucz R.L., 1996, A&A 318, 841
Cavallo R.M., Pilachowski C.A., Rebolo R., 1997, PASP 109, 226
Charbonnel C., 1994, A&A 282, 811
Chmielewski Y., 1984, A&A 133, 83
Clegg R.E.S., Lambert D.L., Tomkin J., 1981, ApJ 250, 262
Clementini G., Carretta E., Gratton R.G., et al., 1995, AJ 110, 2319
Cottrel P.L., Sneden C., 1986, A&A 161, 314
Danylewych L.L., Nicholls R.W., 1978, Proc. R. Soc. London A 360, 557
Denisenkov P.A., Denisenkova S.N., 1990, SvA Lett 16, 275
Dwivedi P.H., Branch D., Huffaker J.N., Bell R.A., 1978, ApJS 36, 573
Edvardsson B., Andersen J., Gustafsson B., et al., 1993, A&A 275, 101 (E93)
Engleman R., Rouse P.E., 1975, JQSRT 15, 831
François P., 1986a, A&A 165, 183
François P., 1986b, A&A 160, 264
Froese-Fisher C., 1975a, Can J. Phys. 53, 184
Froese-Fisher C., 1975b, JOSA 68, 118
Fuhrmann K., 1998, A&A 338, 161
Fuhrmann K., Axer M., Gehren T., 1995, A&A 301, 492
Fulbright J.P., Kraft R.P., 1999, AJ 118, 527
Garstang R.H., 1976, The Airglow and the Aurorae. Pergamon Press, London, p. 324
Gilroy K.K., Brown J.A., 1991, ApJ 371, 578
Gratton R.G., 1990, In: Michaud G., Tutukov A.V. (eds.) IAU Symp. 145, Evolution of Stars: the Photospheric Abundance Connection. Uni. Montreal, Montreal, p. 27
Gratton R.G., Ortolani S., 1986, A&A 169, 201
Gratton R.G., Sneden C., 1987, A&A 178, 179
Gratton R.G., Sneden C., 1988, A&A 204, 193
Gratton R.G., Sneden C., 1991, A&A 241, 501
Gratton R.G., Sneden C., 1994, A&A 287, 927
Gratton R.G., Carretta E., Castelli F., 1996a, A&A 314, 191 (Paper I)
Gratton R.G., Carretta E., Sneden C., Matteucci F., 1996b, In: Morrison H., Sarajedini A. (eds.) Formation of the Galactic Halo... inside and out. ASP Conf. Ser. 92, p. 307
Gratton R.G., Carretta E., Eriksson K., Gustafsson B., 1999, A&A 350, 955 (Paper II)
Gratton R.G., Sneden C., Carretta E., Bragaglia A., 2000a, A&A 354, 169
Gratton R.G., Carretta E., Matteucci F., Sneden C. 2000b, in preparation (Paper IV)
Grevesse, N., Sauval A.J., 1973, A&A 27, 29
Grevesse N., Lambert D.L., Sauval A.J., et al., 1991, A&A 242, 488
Holweger H., 1971, A&A 10, 128
Holweger H., Müller E.A., 1974, Solar Phys. 39, 19
Iben I. Jr., Renzini A., 1983 ARA&A 21, 271
Israelian G., García Lopez R.J., Rebolo R., 1998, ApJ 507, 805
Kaulakys B., 1985, J. Sov. Phys. B: At. Mol. Phys 18, L167
Kaulakys B., 1986, Sov. Phys. JEPT 64, 229
King J.R., 1993, AJ 106, 1206
King J.R., 1994, AJ 107, 350
Kiselman D., 1991, A&A 245, L9
Kiselman D., 1993, A&A 275, 269
Kraft R.P., 1994, PASP 106, 553
Kraft R.P., Suntzeff N.B., Langer G.E., et al., 1982, PASP 94, 55
Kraft R.P., Sneden C., Langer G.E., Prosser C.F., 1992, AJ 104, 645
Kraft R.P., Sneden C., Smith G.H., et al., 1997, AJ 113, 279
Kurucz R.L., 1992, private communication
Kurucz R.L., Furenlid I., Brault J., Tetserman L., 1984, Solar Flux Atlas from 296 to 1300 nm (Harvard, Cambridge)
Kwong H.S., Smith P.L., Parkinson W.H., 1982, Phys. Rev. A 25, 2629
Laird J.B., 1985, ApJ 289, 556
Lambert D.L., 1978, MNRAS 182, 249
Lambert D.L., Luck R.E., 1978, MNRAS 183, 79
Lambert D.L., Ries L.M., 1977, ApJ 217, 508
Lambert D.L., Ries L.M., 1981, ApJ 248, 228
Lambert D.L., Warner B., 1968, MNRAS 138, 181
Langer G.E., Hoffman R., Sneden C., 1993, PASP 105, 301
Luck R.E., 1991, ApJS 75, 579
Magain P., 1987, A&A 179, 176
Magain P., 1989, A&A 209, 211
Matteucci F., François P., 1992, A&A 262, L1
Matteucci F., Greggio L., 1986, A&A 154, 279
Mauas P.J., Avrett E.H., Loeser R., 1988, ApJ 330, 1008
Mendoza C., Zeippen C.J., 1987, A&A 179, 339
Nissen P.E., Edvardsson B., 1992, A&A 261, 255
Nissen P.E., Schuster W.J., 1997, A&A 326, 751
Nissen P.E., Gustafsson B., Edvardsson B., Gilmore G., 1994, A&A 285, 440
Pagel B.E.J., Edmunds M.G., 1981, ARA&A 19, 77
Peterson R.C., Sneden C., 1978, ApJ 225, 913
Pilachowski C.A., Sneden C., Kraft R.P., 1996, AJ 111, 1689
Shetrone M.D., 1996, AJ 112, 1517
Shetrone M.D., Sneden C., Pilachowski C.A., 1993, PASP 105, 337
Simmons G.J., Blackwell D.E., 1982, A&A 112, 209
Sneden C., Lambert D.L., 1982, ApJ 259, 381
Sneden C., Lambert D.L., Whitaker R.W., 1979, ApJ 234, 964
Sneden C., Pilachowski C.A., VandenBerg D.A. 1986, ApJ 311, 826
Sneden C., Kraft R.P., Prosser C.F., Langer G.E., 1991, AJ 102, 2001 (SKPL)
Spiesmann W.J., Wallerstein G., 1991, AJ 102, 1790
Spite M., Spite F., 1991, A&A 252, 689
Steffen M., 1985, A&AS 59, 403
Stürenberg S., Holweger H., 1990, A&A 237, 125
Sweigart A.V., Mengel J.G., 1979, ApJ 229, 624
Thielemann F.K., Hashimoto M., Nomoto K., 1990, ApJ 349, 222
Timmes F.X., Woosley S.E., Weaver T.A., 1995, ApJS 98, 617
Tomkin J., Lambert D.L., 1984, ApJ 279, 220
Tomkin J., Sneden C., Lambert D.L., 1986, ApJ 302, 415
Tomkin J., Lemke M., Lambert D.L., Sneden C., 1992, AJ 104, 1568 (TLLS)
Tomkin J., Woolf V.M., Lambert D.L., Lemke M., 1995, AJ 109, 2204
Truran J.W., 1973, Space Sci. Rev. 15, 23
Truran J.W., Arnett W.D., 1971, A&AS 11, 430
Truran J.W., Cameron A.G.W., 1971, A&AS 14, 179
Tsujimoto T., Nomoto K., Yoshii Y., et al., 1995, MNRAS 277, 945
Twarog B.A., Anthony-Twarog B., 1994, AJ 107, 1577
Wheeler J.C., Sneden C., Truran J.W., 1989, ARA&A 27, 279
Woosley S.E., Weaver T.A., 1986, In: Mihalas D., et al. (eds.) IAU Coll. 89, p. 91
Woosley S.E., Weaver T.A., 1995, ApJS 101, 181
Zhao G., Magain P., 1990, A&A 238, 242 (ZM90)